FEBS Letters 573 (2004) 168–174 FEBS 28732

Hyperosmotically induced accumulation of a phosphorylated p38-like MAPK involved in protoplast volume regulation of plasmolyzed wheat root cells

G. Komis[a], P. Apostolakos[a], C. Gaitanaki[b], B. Galatis[a,*]

[a]*Faculty of Biology, Department of Botany, University of Athens, Athens 157 84, Greece*
[b]*Faculty of Biology, Department of Animal and Human Physiology, University of Athens, Athens 157 84, Greece*

Received 20 July 2004; accepted 28 July 2004

Available online 9 August 2004

Edited by Jesus Avila

Abstract A 46 kDa protein resembling immunochemically to the mammalian dually phosphorylated p38-MAPK was detected in wheat root cells under hyperosmotic conditions, using Western blot analysis. This protein accumulated in a time- and dose-dependent fashion and exhibited pharmacological sensitivity similar to the activated p38-MAPK. The application of a highly specific p38-MAPK inhibitor revealed that the p38-like MAPK is probably implicated in hyperosmotically induced tubulin cytoskeleton reorganization as well as in protoplast volume regulation and osmotic tolerance of wheat root cells. As far as we know, the p38-MAPK has not been previously reported in higher plants.

Keywords: p38-like MAPK; Tubulin cytoskeleton reorganization; Plasmolyzed protoplast volume regulation; *Triticum turgidum*

1. Introduction

MAPKs are key transducers of extracellular stimuli to coordinated cellular responses under various circumstances [1]. MAPKs are discriminated to ERKs, JNKs/SAPK1 and p38/SAPK2. The latter two are associated with stress signaling cascades [1]. Any MAPK cascade may be activated through diverse pathways, including small GTPases [2], heterotrimeric GTPases [3], phosphoinositide [4], cAMP [5], or calcium signaling [6]. Events following MAPK activation diverge from gene expression regulation to the modification of the activity of several cytoplasmic targets, including cytoskeletal proteins [1]. The association of MAPK signaling complexes with cytoplasmic assemblies and specific scaffolding proteins contributes to the spatial specificity and compartmentalization of MAPK signaling [7]. Docking of MAPK complexes to the actin or tubulin cytoskeleton has been reported in other studies [7,8].

In higher plants, MAPK cascades participate in water stress signaling, while more than one MAPK signaling module may be employed at a time [9]. The kind of the activated MAPKs, the accumulated levels of their activated form and the time course pattern of activation depend on either the nature of water stress (hyperosmotic conditions, salinity, drought or cold) [5] or its magnitude [10].

Higher plant MAPKs are classified in to the ERK subgroup [11]. MAPKs similar to animal JNKs or p38, respectively, have not been identified. p38-MAPK is the mammalian homologue of yeast HOG1p MAPK, which is essential for the yeast hyperosmotic response [12]. Since p38-MAPK is conserved from yeast to mammals and holds an elemental role in both early and late events of the hyperosmotic response, we sought its counterparts in angiosperms.

Hereby, we report the detection of a protein sharing immunochemical and pharmacological similarities with the mammalian phosphorylated form of p38-MAPK (phospho-p38-MAPK), which accumulated under hyperosmotic conditions in wheat root cells. Additionally, its involvement in the tubulin cytoskeleton-dependent-mechanism of the protoplast volume regulation previously described in wheat roots [13] was investigated.

2. Materials and methods

2.1. Plant material

Wheat caryopses (*Triticum turgidum* cv. Athos) were imbibed in distilled water for 36–48 h in dark at 25 ± 1 °C. Roots were detached from the seedlings and immersed in MES buffered Hoagland's solution (20 mM MES, pH 5.6, 5 mM $CaCl_2$, 5 mM KNO_3, 2 mM $MgSO_4$, 2 mM KH_2PO_4, 1 μM NaFeEDTA, 0.1 μM each of $NaMoO_4$, $CuSO_4$, $ZnSO_4$, and $MnCl_2$) supplemented with 20 mM glucose. Roots were allowed for 1 h to recover from wounding before the treatments described below.

2.2. Treatments

Hyperosmotic conditions were achieved with 1 M sucrose in Hoagland's medium. For time course experiments, hyperosmotically stressed roots were sampled at 10, 30, 60, 90, 120, 240 and 480 min after the onset of the hyperosmotic stress and processed for either immunofluorescence or Western blotting. For dose–response experiments, samples were exposed to different concentrations of the hyperosmotic medium for 1 h. For inhibitor treatments, roots were treated with MAPK inhibitors for 2 h before and for 1 h during the hyperosmotic stress.

MAPK signaling was impaired by the use of PD98059 (MEK1 inhibitor, Calbiochem), U0126 (MEK1/2 inhibitor, Calbiochem), or SB203580 (p38-MAPK inhibitor, Calbiochem). All inhibitors were prepared as 10 mM stock solutions in DMSO. The solvent alone had no effect on the phosphorylation of the p38-MAPK under the conditions used. To test the efficacy of PD98059 to inhibit the accumulation

* Corresponding author.
E-mail address: bgalatis@biol.uoa.gr (B. Galatis).

0014-5793/$22.00
doi:10.1016/j.febslet.2004.07.065

of the phosphorylated plant ERK species, excised roots were treated for 30 min with 1 μM phorbol 12-myristate 13-acetate (PMA) in Hoagland's solution in the presence or absence of 25 μM PD98059. PMA-induced plant ERK activation was previously documented [14].

2.3. Western blotting

Roots treated as described above were washed with ice-cold phosphate buffered saline (PBS) and homogenized with 1 volume of ice-cold extraction buffer (100 mM K-HEPES, pH 7.5, 50 mM β-glycerophosphate, 10 mM EGTA, 10 mM DTT, 20 mM NaF, 150 mM NaCl, 20% (v/v) glycerol, 1% (v/v) Triton X-100, 1 mM Na_3VO_4, 1 mM Pefabloc and 1 tablet of the Mini Complete protease inhibitor cocktail). The homogenate was clarified at $6000 \times g$ for 10 min at 2 °C. The supernatants were mixed proportionally with Laemmli sample buffer and subjected to SDS–PAGE. Approximately, 100 μg of protein was loaded per well. Protein content was determined by the micro BCA kit (Pierce). Gels were semi-dry blotted to nitrocellulose sheets (Protran Schleicher and Schuell). Membranes were blocked with 1% (w/v) BSA in Tris-buffered saline plus 0.1% (v/v) Tween 20 (TBST) for 1 h at room temperature and successively treated with the adequate primary antibody (see below) overnight at 4 °C and HRP-conjugated secondary antibody (DAKO HRP-anti-rabbit or HRP-anti-mouse) for 1 h at room temperature. Membranes were then developed with the ECL reagent kit (Amersham Biosciences) according to the manufacturer's instructions and exposed to Kodak XOMAT films. MAPK or tubulin probed blots were quantified by scanning densitometry using Gel Analyzer software. Statistical analysis was done with Graph Pad Prizm 4.0 software.

2.4. Antibodies

The dually phosphorylated form of p38-MAPK was probed using an affinity purified polyclonal serum developed against a synthetic peptide corresponding to the dually phosphorylated epitope of the p38-MAPK (Cell Signaling, Cat. No. 9211), diluted 1:1000 in TBST with 5% (w/v) BSA. Total p38 was detected with a rabbit polyclonal antibody (Cell Signaling, Cat. No. 9212) diluted 1:250 in TBST with 5% (w/v) BSA. Phospho-ERKs were probed with rabbit polyclonal antibodies (Cell Signaling, Cat. No. 9101 and Santa Cruz, Cat. No. SC16982) diluted 1:1000 in TBST with 5% (w/v) BSA. To ensure equal loading per well, membranes were stripped and reprobed with the mouse monoclonal anti-α-tubulin antibody DM1A (Sigma) diluted 1:250 in TBST with 5% (w/v) BSA.

2.5. Immunofluorescence

For immunolabeling of tubulin polymers, root tips were fixed in 8% (w/v) paraformaldehyde in microtubule (Mt) stabilizing buffer (MSB; 100 mM K-PIPES, pH 6.8, 5 mM EGTA and 10 mM $MgSO_4$). Cell walls were digested with 1% (w/v) driselase, 3% (w/v) cellulase Onozuka R-10, 1% (w/v) macerozyme and 3% (w/v) pectinase and root tips were macerated on polycationized acid-washed coverslips to release individual cells. These were successively permeabilized with 3% (v/v) Triton X-100 in PBS, pH 7.4, blocked with 3% (w/v) BSA in PBS and probed with an anti-α-tubulin monoclonal antibody (clone YOL1/34, Abcam, diluted 1:100 in PBS) and finally with FITC-conjugated anti-rat IgGs (Sigma, diluted 1:20 in PBS).

Nuclei were counterstained with bis-benzimide (Hoechst 33258, Sigma) and specimens were mounted in 90% (v/v) glycerol in PBS, pH 8.0, supplemented with 0.1% (w/v) of paraphenylenediamine as an antifading agent. Specimens were observed and photographed through a Zeiss Axioplan microscope equipped with Neofluar objectives and standard monochromatic filters. Photomicrographs were captured on Kodak T-MAX 400 film rated at 1600 ISO.

2.6. Transmission electron microscopy and tubulin polymer morphometric analysis

Root tips were fixed, dehydrated, infiltrated and embedded in Spurr's resin as previously described [13]. Thin sections were sequentially stained with uranyl acetate and lead citrate and observed through a Philips 300 EM. For Mts and macrotubule diameter measurements, the microscope was calibrated with a grated microscale and measurements were conducted accordingly [13].

2.7. Microscopic assessment of living material

Paradermal sections of MAPK inhibitor-treated or untreated roots were collected in a drop of 1 M sucrose in Hoagland's solution with or without inhibitors and studied through time using DIC optics. Protoplast volume measurements were conducted using Hoffler's method [13].

3. Results

3.1. General remarks on the hyperosmotically treated cells

The time course of plasmolysis of wheat root cells in hyperosmotic sucrose was essential as described for mannitol

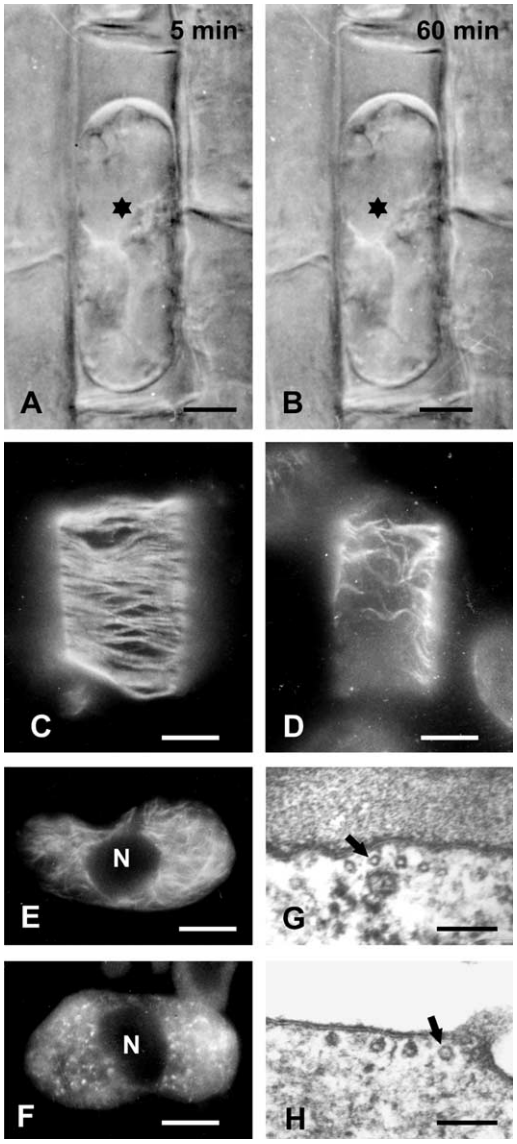

Fig. 1. Plasmolyzed root cells under DIC optics (A, B), after tubulin immunofluorescence (C–F) and in TEM (G, H). (A, B) DIC micrographs of a living rhizodermal cell treated with 1 M sucrose for 5 and 60 min. The asterisks mark the plasmolyzed protoplast. The protoplast volume remains almost the same after 60 min of plasmolysis. Bars 10 μm. (C) Cortical macrotubule arrays in a root cell plasmolyzed with 1 M sucrose for 30 min. Bar 10 μm. (D) Root cell treated with 1 μM SB203580 for 2 h and exposed to 1 M sucrose supplemented with 1 μM SB203580 for 60 min, showing poor development and abnormal distribution of cortical tubulin strands (compare with figure C). Bar 10 μm. (E) Perinuclear macrotubule arrays in a root-cap cell plasmolyzed with 1 M sucrose for 30 min. Bar 10 μm. (F) Root-cap cell treated as the cell of figure D, lacking tubulin strands (compare with figure E). Bar 10 μm. (G, H) Electron micrographs of cross-sectioned Mts (G, arrow) and macrotubules (H, arrow). Bar 100 nm.

solutions [13]. In untreated roots, plasmolysis was concluded within 5–10 min after the exposure of root cells to the hyperosmotic medium. At longer times, no significant changes in the volume of the plasmolyzed protoplast were observed (Fig. 1A and B). In their vast majority, the plasmolyzed protoplasts assumed a convex form (Fig. 1A and B).

In plasmolyzed interphase cells, Mts were replaced by thick strands of tubulin polymers, traversing the cortical cytoplasm and the endoplasm (Fig. 1C and E). TEM observations revealed that the tubulin strands consist of macrotubules (Fig. 1H; cf. Fig. 1G) with a diameter ranging from 24 to 33 nm (mean diameter 27 ± 0.3 nm, $n = 102$). In contrast, the mean Mt diameter in control cells was 21 ± 0.4 nm ($n = 105$). Differences between the mean diameters (macrotubules vs Mts) were statistically significant ($P < 0.05$). The macrotubules in the plasmolyzed plant cells consist probably of more than 13 protofilaments [13,14].

3.2. Hyperosmotic conditions induce the accumulation of a phospho-p38-like MAPK in a time- and dose-dependent manner

Western blot localization of a 46 kDa phospho-p38-like MAPK in extracts collected from a time series in 1 M sucrose yielded a time-dependent pattern of accumulation. The accumulation of this protein started as early as 10 min from the onset of hyperosmotic treatment and peaked 90–120 min later (Fig. 2B).

Densitometric analysis showed that phospho-p38 immunoreactivity started to accumulate as soon as 10 min after the onset of the hyperosmotic treatment and increased up to 900% at 120 min compared with the control (Fig. 2A). During longer exposure of seedlings to the hyperosmotic medium, the levels of phospho-p38 drop yet remaining higher than the levels of phospho-p38-like MAPK of control cell extracts (Fig. 2A and B). Total p38 immunoreactivity as probed in appropriate Western blots (Fig. 2B) remained fairly constant in root cell extracts at the same time series of 1 M sucrose treatment.

For dose–response experiments, roots were treated with the hyperosmotic solutions at the concentrations indicated in Fig. 3 for 1 h. Increase in phospho-p38 immunoreactivity was also found in roots subjected to sucrose concentrations as low as 250 mM (Fig. 3A and B), where no plasmolysis was microscopically detectable. At increasing sucrose concentrations, the levels of phospho-p38 immunoreactivity were proportionally enhanced (Fig. 3A and B) and reached saturation at 1 M sucrose (Fig. 3A).

Mechanical wounding due to detachment of roots from the seedlings had no effect on the accumulation of the phospho-p38 MAPK immunoreactivity (data not shown).

To test whether the detection of phospho-p38-like MAPK was due to cross reactivity of the antibody used hereby with phospho-ERK species, blots of hyperosmotically treated root cell extracts were analyzed with two anti-phospho-ERK antibodies (see Section 2.4). As it is shown in Fig. 4A and B, the phospho-ERKs are absent from the plasmolyzed root extracts.

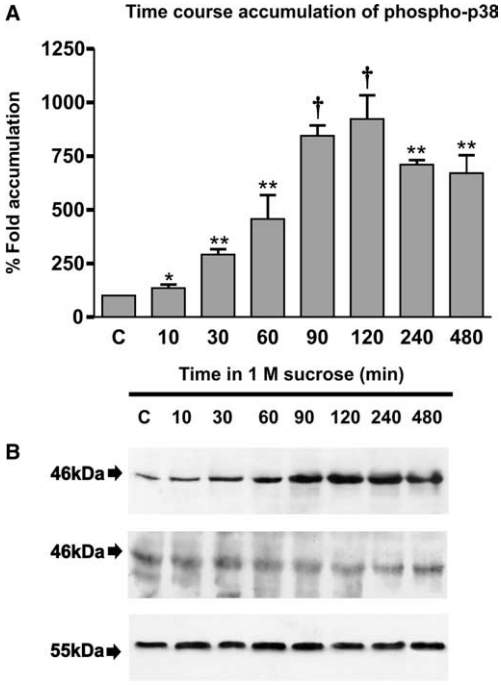

Fig. 2. Time-dependent accumulation of phospho- and total p38 immunoreactivity in roots challenged by 1 M sucrose in Hoagland's solution. (A) Quantification of root extracts collected at the designated time points for phospho-p38 immunoreactivity (mean % fold accumulation ± S.E.M. from 4 independent experiments, $*P < 0.05$, $**P < 0.01$, $^{\dagger}P < 0.001$ vs control value). Control (C) was arbitrarily set as 100%. (B) Western blots demonstrating the time course of phospho-p38 (upper) and total p38 (middle) immunoreactivity accumulation as well as the respective loading control probed with the DM1A anti-tubulin mAb (lower). Total p38 MAPK or DM1A lane-to-lane density fluctuation is not statistically significant ($P > 0.1$).

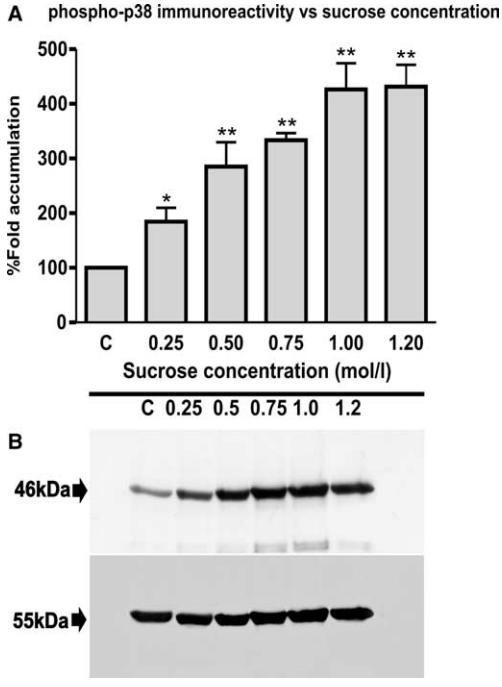

Fig. 3. Dose-dependent accumulation of phospho-p38 immunoreactivity of root extracts treated with the designated sucrose concentrations in Hoagland's solution. (A) Quantification of root cell extracts treated for 1 h with different sucrose concentrations (mean % fold accumulation ± S.E.M. from 4 independent experiments, $*P < 0.05$, $**P < 0.01$ vs control value). Control (C) was arbitrarily set as 100%. (B) Western blots demonstrating the dose–response of phospho-p38 immunoreactivity (upper) and the respective loading control probed with the DM1A anti-tubulin mAb (lower).

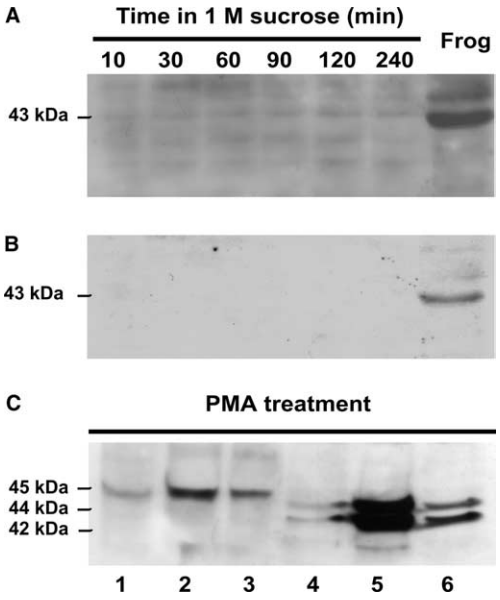

Fig. 4. Roots treated with 1 M sucrose for the designated time series (A, B) or with 1 μM PMA in the presence or absence of 25 μM PD98059 (C) and probed with anti-phospho-ERK antibodies. (A, B) The same Western blot probed with either the Cell Signaling antibody (A) or Santa Cruz antibody (B) showing phospho-ERK absence. In the last lane, a positive control from hyperosmotically treated frog heart is included. (C) Western blot demonstrating phospho-ERK immunoreactivity of extracts from control roots (1), roots treated with 1 μM PMA (2) and roots treated with 1 μM PMA in the presence of 25 μM PD98059 (3). In lanes 4, 5, and 6, mammalian C2 mouse skeletal myoblasts treated likewise were included as positive controls for phospho-ERK immunoreactivity. Obviously, the antibody used hereby detects phospho-ERK (1, 2, 3) and PD98059 inhibits the phospho-ERK accumulation (lane 3; cf. lane 2) in our system.

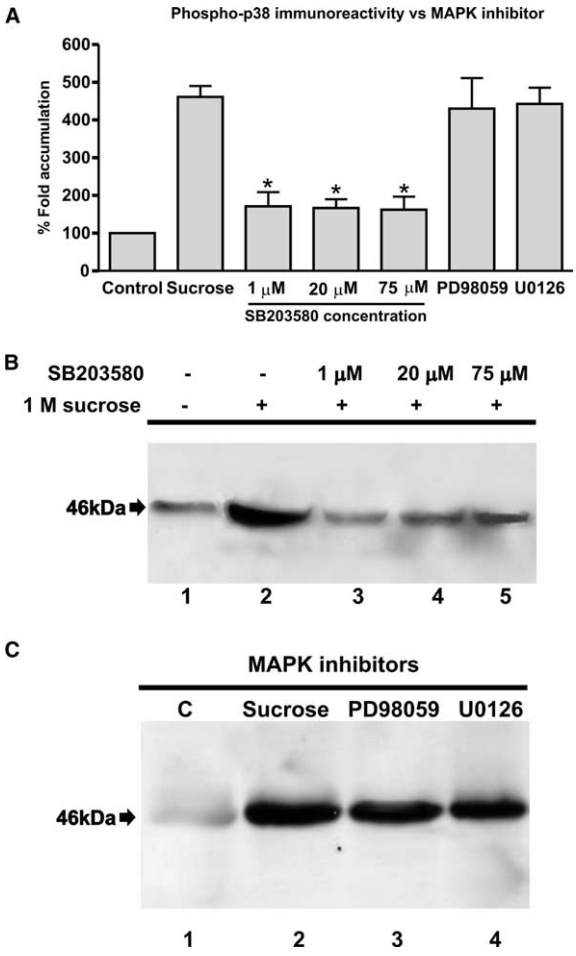

Fig. 5. Differential effects of three MAPK inhibitors on the sucrose-induced accumulation of phospho-p38 immunoreactivity. (A) Quantification of sucrose-induced phospho-p38 immunoreactivity in the absence or presence of SB203580 (1, 20 and 75 μM), PD98059 (50 μM) and U0126 (50 μM). Results are depicted as mean % fold accumulation ± S.E.M. from 4 independent experiments (*$P < 0.05$ vs sucrose value). Control (C) was arbitrarily set as 100%. (B) Western blot to demonstrate the phospho-p38 immunoreactivity of extracts from control roots (1) and roots treated with 1 M sucrose (2) or with 1 M sucrose plus 1, 20 and 75 μM SB203580 (3–5). (C) Western blot demonstrating the phospho-p38 immunoreactivity of extracts from control roots (1) and roots treated with 1 M sucrose (2) and with 1 M sucrose plus 50 μM PD98059 (3), or 50 μM U0126 (4).

In contrast, both antibodies detected a very prominent band at approximately 45 kDa in extracts from control (non-plasmolyzed) roots treated with the ERK activator PMA (Fig. 4C). This finding shows that both antibodies have the ability to recognize phospho-ERKs (see also [15]). Furthermore, the MEK1 selective inhibitor PD98059 (25 M) abolished the ERK activation induced by PMA (Fig. 4C).

3.3. Effects of MAPK inhibitors on the hyperosmotically induced accumulation of the phospho-p38-like MAPK

Western blot analysis of samples from hyperosmotically treated roots incubated along with the p38-MAPK specific inhibitor SB203580 revealed a dramatic reduction (270% with respect to sucrose treated roots) in the levels of phospho-p38 immunoreactivity at micromolar concentrations (1–75 μM, Fig. 5A and B). SB203580 is a highly selective inhibitor of the activated phosphorylated form of p38-MAPK. However, it has been repeatedly reported to also prevent the phosphorylation of the inactive p38-MAPK by interfering with the interaction of the p38-MAPK with its upstream activators [16]. Concerning other inhibitors, neither PD98059 nor U0126, both used at 50 μM, inhibited the accumulation of phospho-p38 immunoreactivity under hyperosmotic conditions (Fig. 5A and C).

3.4. The effects of MAPK inhibitors on the course of plasmolysis and the volume of the plasmolyzed protoplast

To assess the role of MAPKs in the osmotic tolerance of plasmolyzed wheat root cells against hyperosmotic conditions, roots were exposed to hypertonic sucrose solutions in the presence of MAPK inhibitors SB203580, PD98059 or U0126. In all cases, root cells were monitored for up to 2 h. Finally, roots plasmolyzed in the presence or absence of inhibitors, were fixed and the volumes of the plasmolyzed protoplasts were measured accordingly [13].

Treatment of roots with either 20 μM PD98059, or 20 μM U0126, both inhibitors of the ERK pathway, did not have any significant effect on the time course of plasmolysis. The chain of events during the exposure of PD98059 or U0126-treated root cells was almost identical to that of the untreated ones (data not shown). By contrast, SB203580 had profound effects even at 1 μM. In this case, plasmolysis was significantly prolonged as the protoplast volume diminution continued for up to 1 h after the exposure of root cells to the hyperosmotic medium (Fig. 6A and B; cf. Fig. 1A and B).

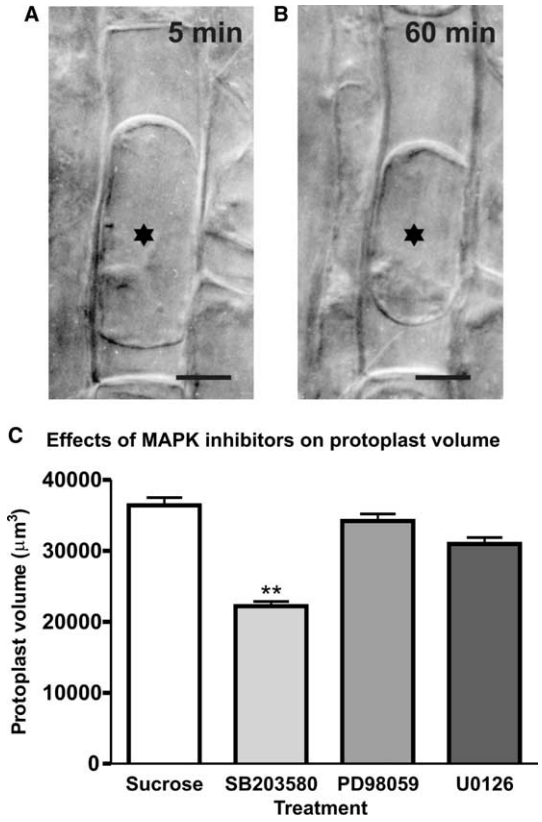

Fig. 6. (A, B) DIC micrographs of living rhizodermal cells pretreated with 1 μM SB203580 for 2 h taken at 5 and 60 min after treatment with 1 M sucrose plus 1 μM SB203580. Volume reduction of the plasmolyzed protoplasts (asterisks) is evident. Bar 10 μm. (C) Histogram depicting the mean protoplast volumes (±S.E.M.) of rhizodermal cells treated with 1 M sucrose for 60 min or treated for the same time with 1 M sucrose plus 1 μM SB203580, or 20 μM PD98059 or 20 μM U0126. Differences of mean protoplast volume between sucrose-treated and sucrose plus SB203580 treated cells were statistically significant (**$P < 0.01$).

Volume measurements of the plasmolyzed protoplast revealed that either PD98059 or U0126 treatments did not have any statistically significant effect (Fig. 6C). By contrast, SB203580 treatment brought about approximately 45% diminution of the plasmolyzed protoplast volume when compared to untreated plasmolyzed cells (Fig. 6C).

3.5. The effects of MAPK inhibitors on the hyperosmotically induced tubulin cytoskeleton reorganization

Since tubulin cytoskeleton reorganization holds a pivotal role in the osmotic tolerance of wheat root cells [13], we reasoned that the phospho-p38-like protein could be involved to some extent in the formation and/or organization of hyperosmotically induced tubulin macrotubules. For this purpose, we studied the organization of tubulin cytoskeleton in hyperosmotically treated root cells in the presence of the MAPK inhibitors SB203580 or PD98059.

Non-plasmolyzed root cells exposed to either 1 μM SB203580, or 20 μM PD98059 for 3 h were processed for tubulin immunofluorescence to test whether the inhibitors exert any effect on Mt organization. In both cases, cortical Mt arrays were normal (data not shown).

SB203580 treatment of root cells exposed to 1 M sucrose yielded a tubulin cytoskeletal response markedly different from that expected under typical hyperosmotic conditions. Usually, the SB203580-treated interphase plasmolyzed cells display sparsely arranged atypical strands of cortical tubulin polymers instead of the dense and diffuse macrotubule arrays expected (Fig. 1D; cf. Fig. 1C), or they lack tubulin strands. The latter phenomenon is clear in the plasmolyzed root-cap cells, where radial perinuclear macrotubule arrays are typically observed. SB203580 treatment induced their disappearance from every cell examined (Fig. 1F; cf. Fig. 1E). PD98059 treatment did not affect the hyperosmotically induced tubulin cytoskeleton reorganization (data not shown).

TEM examination of cells plasmolyzed in the presence of 1 μM SB203580 confirmed in their majority the low abundance of tubulin polymers, while in few, which were not intensely plasmolyzed, those persisted forming clusters (data not shown).

4. Discussion

4.1. Identification of a phosphorylated p38-like MAPK in hyperosmotically stressed cells

The most significant finding presented hereby is the detection of a 46 kDa phospho-p38-like MAPK in hyperosmotically stressed root cells of an angiosperm for the first time. So far, p38-like and JNK-like MAPKs have been excluded from higher plants based on sequence analysis failure to recover plant homologues of TGY and TPY motifs within the activation loop of MAPKs [11]. However, recently, Jimenez et al. [17] demonstrated the occurrence of a 57 kDa phospho-p38-like MAPK in hyperosmotically and UV-stressed unicellular alga *Dunaliella*. In our system, detection of the phospho-p38-like MAPK was based on a highly specific antibody raised against the phosphorylated form of an oligopeptide containing the ^{180}TG^{182}Y motif of mammalian p38-MAPK. This antibody detected phospho-p38-MAPK in phylogenetically distant organisms including algae [17], mammals [18], amphibians [19,20] and mussels [21]. Additionally, antibodies raised against the similar oligopeptide of mammalian ERKs failed to detect the 46 kDa band in the plasmolyzed root cells of wheat (Fig. 4A and B), suggesting that there was no false cross-reactivity with the ERK species. The most compelling evidence, however, comes from the use of SB203580, a highly specific p38-MAPK activation inhibitor [15]. Plasmolysis in the presence of SB203580 resulted in the dramatic diminution of the phospho-p38-like MAPK levels in immunoblots.

4.2. Probable involvement of the p38-like MAPK in tubulin cytoskeleton reorganization and protoplast volume regulation

In plants, hyperosmotic stress induces massive reorganization of the tubulin and actin cytoskeleton [13,14,22–25]. In wheat root cells, Mts are disintegrated and replaced by tubulin macrotubules [13]. In contrast, in hyperosmotically stressed *Chlorophytum comosum* leaf cells, an extensive reorganization of the actin cytoskeleton occurs [25]. Results from the present study, revealed that a SB203580 sensitive mechanism interferes with Mt disintegration and/or macrotubule polymerization. Since SB203580 is a highly specific inhibitor of the p38-MAPK [15], it is reasonable to assume that the phospho-p38-like

MAPK identified in this work is related to this mechanism. Although the implication of MAPKs in mechanisms controlling cytoskeletal organization and dynamics has been demonstrated in plants, the involvement of a p38-MAPK has not been reported so far. In alfalfa suspension culture cells, a stress activated MAPK (SAMK), is responsive against antimicrotubular treatments and becomes activated by the use of either oryzalin or low temperatures [26]. In salt stressed alfalfa root cells, the MAPK SIMK colocalizes with the preprophase Mt band, the mitotic spindle and the phragmoplast but not with the interphase cortical Mt arrays [27,28]. Two other MAPKs, NPK1 and NtF6 identified in cytokinetic tobacco cells, are involved in the formation and development of the phragmoplast [27].

In animal cells, p38-MAPK is directly involved in Mt organization and function. In human gingival fibroblasts and rat2 cells, mechanical loading induces both the activation of p38-MAPK and its translocation to the focal adhesion sites in a Mt-dependent manner [29]. Besides, in hypo-osmotically treated rat liver cells, Mts mediate autophagosome formation downstream of p38-MAPK activation [30]. The relationship between p38-MAPK activation and the tubulin polymer state is furthermore substantiated in studies of animal cells demonstrating differential effects of various anti-cytoskeletal drugs on p38-MAPK activation [31]. Among the possible targets of p38-MAPK relevant to Mt dynamics and organization stathmin and tau proteins are included [1]. Mt-p38-MAPK interactions are also implicated in the spatial control of p38-MAPK signaling, while scaffolding proteins like JIP2, link p38-MAPK to Mts via interactions with kinesin motor proteins [7]. This information supports the view that the 46 kDa phospho-p38-like MAPK is involved in the control of tubulin cytoskeleton reorganization in the plasmolyzed wheat root cells.

In plants, Mts may be involved in the guard cell volume regulation occurring in stomatal movement, being probably required upstream to the H^+ efflux and K^+ influx leading to stomatal movement (reviewed in [32]). In the plasmolyzed wheat root cells, tubulin macrotubules appear involved in a protoplast volume regulatory mechanism [13]. The present findings revealed that a p38-like MAPK signaling pathway is probably implicated in the above mechanism cooperating with the cortical macrotubules, as assessed by the use of SB203580. This phospho-p38-MAPK inhibitor interfered with the osmotic tolerance of wheat root cells and the state of the tubulin polymers.

In animals, although Mt arrays seem to be implicated in the regulatory volume increase (RVI) [33], this phenomenon is functionally coupled to the actin cytoskeleton remodeling involved in both the regulation of ionic transport and plasma membrane protection. Two prominent features of RVI, the induction of polymerization of actin filaments and their interaction with NHE1, are in part controlled by the activated p38-MAPK. The mechanism through which p38-MAPK affects actin polymer fraction depends on the p38-MAPK mediated Hsp27 phosphorylation [34]. p38-MAPK is also involved in another major aspect of RVI, the regulation of sodium/proton exchange through the function of plasma membrane NHEs and particularly NHE1, which is ubiquitously involved in RVI events [35]. The hyperosmotic activation of NHE1 by phosphorylation has been partially attributed to p38-MAPK activation [36]. Since NHE1 regulation also depends on components of the actin cytoskeleton [37], the role of p38-MAPK in its regulation might be more complex.

SIMK was initially identified as a plant MAPK activated in a wide range of osmotic stress [10]. SIMK is also related to the actin-dependent root-hair tip growth [38]. Considering that the actin cytoskeleton appears to be involved in the control of protoplast volume in plasmolyzed leaf cells of *Chlorophytum comosum* [25,39], it would be interesting to find out whether SIMK and/or a p38-like MAPK are implicated in the hyperosmotically induced actin filament reorganization [25,39].

Acknowledgements: This work was funded by a Pythagoras research grant (Ministry of Education). The authors also thank Drs C. Komis, E. Dotsica and K. Karagouni (Hellenic Pasteur Institute) for their help and Dr M. Zachariadis for preparation of the plates of this article.

References

[1] Chen, Z., Gibson, T.B., Robinson, F., Silvestro, L., Pearson, G., Xu, B., Wright, A., Vanderbilt, C. and Cobb, M.H. (2001) Chem. Rev. 101, 2449–2476.
[2] Gallagher, E.D., Gutowski, S., Sternweis, P.C. and Cobb, M.H. (2004) J. Biol. Chem. 279, 1872–1877.
[3] Xiong, L., Schumaker, K.S. and Zhu, J.K. (2002) Plant Cell 14 (Suppl.), S165–S183.
[4] Munnik, T. and Meijer, H.J. (2001) FEBS Lett. 498, 172–178.
[5] Sun, B., Ma, H. and Firtel, R.A. (2003) Mol. Biol. Cell 14, 4526–4540.
[6] Agell, N., Bachs, O., Rocamora, N. and Villalonga, P. (2002) Cell Signal 14, 649–654.
[7] Morrison, D.K. and Davis, R.J. (2003) Annu. Rev. Cell Dev. Biol. 19, 91–118.
[8] Uhlik, M.T., Abell, A.N., Johnson, N.L., Sun, W., Cuevas, B.D., Lobel-Rice, K.E., Horne, E.A., Dell'Acqua, M.L. and Johnson, G.L. (2003) Nature Cell Biol. 5, 1104–1110.
[9] Droillard, M., Boudsocq, M., Barbier-Brygoo, H. and Lauriere, C. (2002) FEBS Lett. 527, 43–50.
[10] Munnik, T., Ligterink, W., Meskiene, I.I., Calderini, O., Beyerly, J., Musgrave, A. and Hirt, H. (1999) Plant J. 20, 381–388.
[11] Tena, G., Asai, T., Chiu, W.L. and Sheen, J. (2001) Curr. Opin. Plant Biol. 4, 392–400.
[12] Gustin, M.C., Albertyn, J., Alexander, M. and Davenport, K. (1998) Microbiol. Mol. Biol. Rev. 62, 1264–1300.
[13] Komis, G., Apostolakos, P. and Galatis, B. (2002) Plant Cell Physiol. 43, 911–922.
[14] Komis, G., Apostolakos, P. and Galatis, B. (2001) New Phytol. 149, 193–207.
[15] Baudouin, E., Charpenteau, M., Ranjeva, R. and Ranty, B. (2002) Planta 214, 400–405.
[16] Frantz, B., Klatt, T., Pang, M., Parsons, J., Rolando, A., Williams, H., Tocci, M.J., O'Keefe, S.J. and O'Neill, E.A. (1998) Biochemistry 37, 13846–13853.
[17] Jimenez, C., Berl, T., Rivard, C.J., Edelstein, C.L. and Capasso, J.M. (2004) Biochim. Biophys. Acta 1644, 61–69.
[18] phospho-p38 MAP kinase (Thr180/Tyr182) antibody datasheet. Cell Signaling Technology Inc. Available from: http://www.cell-signal.com/pdf/9211.pdf.
[19] Aggeli, I.K., Gaitanaki, C., Lazou, A. and Beis, I. (2001) Am. J. Physiol. 281, R1689–R1698.
[20] Aggeli, I.K., Gaitanaki, C., Lazou, A. and Beis, I. (2002) J. Exp. Biol. 205, 443–454.
[21] Gaitanaki, C., Kefaloyanni, E., Marmari, A. and Beis, I. (2004) Mol. Cell Biochem. 260, 119–127.
[22] Blancaflor, E.B. and Hasenstein, K.H. (1995) Int. J. Plant Sci. 156, 774–783.
[23] Lang-Pauluzzi, I. and Gunning, B.E.S. (2000) Protoplasma 212, 174–185.
[24] Cleary, A.L. (2001) Protoplasma 215, 21–34.
[25] Komis, G., Apostolakos, P. and Galatis, B. (2002) J. Exp. Bot. 53, 1699–1710.
[26] Sangwan, V., Orvar, B.L., Beyerly, J., Hirt, H. and Dhindsa, R.S. (2002) Plant J. 31, 629–638.
[27] Šamaj, J., Baluška, F. and Hirt, H. (2004) J. Exp. Bot. 55, 189–198.

[28] Baluška, F., Ovecka, M. and Hirt, H. (2000) Protoplasma 212, 262–267.
[29] D'Addario, M., Arora, P.D., Ellen, R.P. and McCulloch, C.A. (2003) J. Biol. Chem. 278, 53090–53097.
[30] vom Dahl, S., Dombrowski, F., Schmitt, M., Schliess, F., Pfeifer, U. and Haussinger, D. (2001) Biochem. J. 354, 31–36.
[31] Stone, A.A. and Chambers, T.C. (2000) Exp. Cell. Res. 254, 110–119.
[32] Galatis, B. and Apostolakos, P. (2004) New Phytol. 161, 613–639.
[33] Moustakas, A., Theodoropoulos, P.A., Gravanis, A., Haussinger, D. and Stournaras, C. (1998) Contrib. Nephrol. 123, 121–134.
[34] Concannon, C.G., Gorman, A.M. and Samali, A. (2003) Apoptosis 8, 61–70.
[35] Szaszi, K., Grinstein, S., Orlowski, J. and Kapus, A. (2000) Cell Physiol. Biochem. 10, 265–272.
[36] Roger, F., Martin, P.Y., Rousselot, M., Favre, H. and Feraille, E. (1999) J. Biol. Chem. 274, 34103–34110.
[37] Pedersen, S.F., Hoffmann, E.K. and Mills, J.W. (2001) Comp. Biochem. Physiol. A 130, 385–399.
[38] Šamaj, J., Ovecka, M., Hlavacka, A., Lecourieux, F., Meskiene, I., Lichtscheidl, I., Lenart, P., Salaj, J., Volkmann, D., Bögre, L., Baluška, F. and Hirt, H. (2002) EMBO J. 21, 3296–3306.
[39] Komis, G., Apostolakos, P. and Galatis, B. (2003) Protoplasma 221, 245–256.